

Electronic Supplementary Information

Comprehensive Utilization Strategy of Cellulose in a Facile, Controllable, High-Yield Preparation Process of Cellulose Nanocrystals Using Aqueous Tetrabutylphosphonium Hydroxide

Fangchao Cheng^{a,b,}, Panpan Zhao^a, Tulong Ouyang^a, Jianping Sun^a, Yiqiang Wu^{b,*}*

^a Guangxi Key Laboratory of Processing for Nonferrous Metallic and Featured Materials, School of Resources, Environment and Materials, Guangxi University, Nanning 530004, China

^b College of Material Science and Engineering, Central South University of Forestry and Technology, Changsha 410004, China

*Corresponding authors: fangchaocheng@gxu.edu.cn; wuyq0506@126.com

Effects of temperature, solid-liquid ratio, time, ultrasonic power and raw material on the CNC yield

Treatment temperature, as one of the important factors that can regulate the acid hydrolysis process for CNC preparation, can greatly affect the hydrolysis rate of cellulose and the CNC yield.¹ Different from the acid hydrolysis method, in the current method, the CNC yield obtained with a solid-liquid ratio of 0.05:1 at the selected temperatures (40, 50 and 60 °C in Experiments 4, 5, and 6 in Table S1) of this study showed no significant difference, which was mainly attributed to the highly efficient cellulose dissolution capacity of TBPH solution.² Nevertheless, the increase in the treatment temperature can enhance the CNC preparation when increasing the solid-liquid ratio to 0.1:1, and the higher solid-liquid ratio led to an obvious decrease in the CNC yield. This was mainly because higher MCC loading can result in higher viscosity of the TBPH/cellulose solution,³ which hindered the effective disassembly of cellulose. Elevated temperature would lead to lower viscosity of the system, thus enhancing the CNC preparation.

The extension of the treatment time from 30 min to 60 min also showed a beneficial effect on the CNC yield, while further extension to 80 min resulted in an obvious decrease in the yield. As reported previously, 60 wt% TBPH solution enabled the dissolution of cellulose,³ and a significantly lower TBPH concentration of 40 wt% was found to be favorable to the CNC preparation in this study. In this case, cellulose cannot be completely dissolved in the system,

and a longer duration allowed more hydrogen bonds of cellulose to be disassembled. Nevertheless, further time extension would result in more cellulose dissolution and thus lower CNC yield.

The present method showed promising tunability in the ultrasonic power requirement, and an ultrasonic power as low as 400 W can still give a desirable CNC yield of 49.6%. The increase in ultrasonic power from 400 W to 1200 W can effectively enhance the dispersion of regenerated cellulose and CNC preparation, while a higher ultrasonic power (1600 W) led to a lower CNC yield. As reported previously, proper ultrasonic treatment can effectively enhance the accessibility of the cellulose amorphous region,⁴ which is conducive to nanocellulose generation.

Additionally, a high CNC yield of 70.2 wt% can also be achieved in the preparation process using bleached pulp as raw materials under the optimal conditions (Experiment 16, Table S1). Compared to the process using MCC as raw materials, the pulp-related process led to a slightly lower yield, which may be attributed to the slightly higher lignin content (1.9% vs. 0.7%), the larger molecular weight and recalcitrant crystalline structure of the bleached pulp.⁵

Table S1. Results of CNC yield under different conditions

Experiment	Concentration (wt%)	Temperature (°C)	Ultrasonic Power (W)	Time (min)	Solid- liquid Ratio	Yield (%)
1	30	50	1200	60	0.05:1	28.2±0.4
2	40	50	1200	60	0.05:1	72.2±5.0
3	50	50	1200	60	0.05:1	43.7±2.2
4	60	50	1200	60	0.05:1	28.7±6.7
5	40	40	1200	60	0.05:1	66.7±2.0
6	40	60	1200	60	0.05:1	70.3±2.6
7	40	50	400	60	0.05:1	49.6±8.3
8	40	50	800	60	0.05:1	62.2±6.0
9	40	50	1600	60	0.05:1	67.9±4.8
10	40	50	1200	30	0.05:1	61.2±13.3
11	40	50	1200	40	0.05:1	64.4±2.1
12	40	50	1200	80	0.05:1	55.7±9.9
13	40	40	1200	60	0.1:1	39.1±10.1
14	40	50	1200	60	0.1:1	46.0±8.1
15	40	60	1200	60	0.1:1	52.5±6.1
16 (Pulp CNC)	40	50	1200	60	0.05:1	70.2±2.3

Morphology analysis

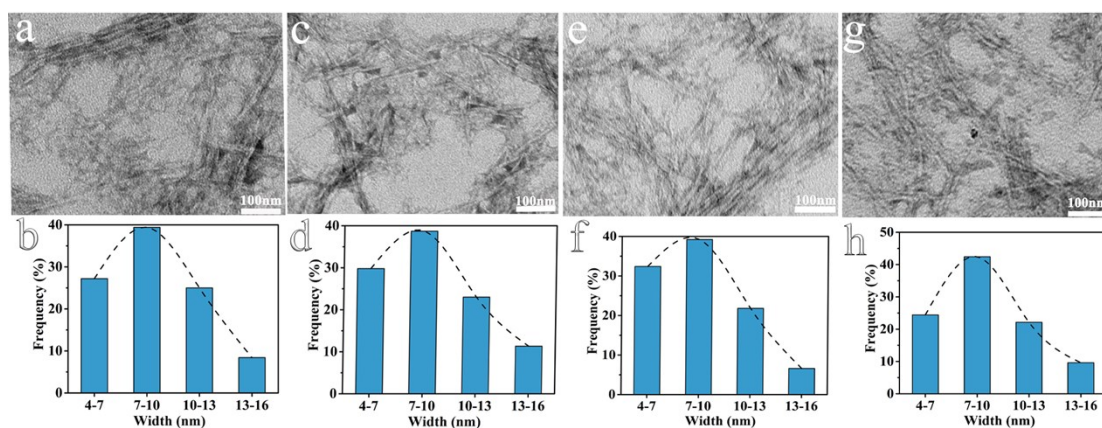


Figure S1. TEM images and diameter distributions of CNC and pulp CNC samples: (a-b) NC40°C; (c-d) NC50°C; (e-f) NC60°C; (g-h) Pulp CNC.

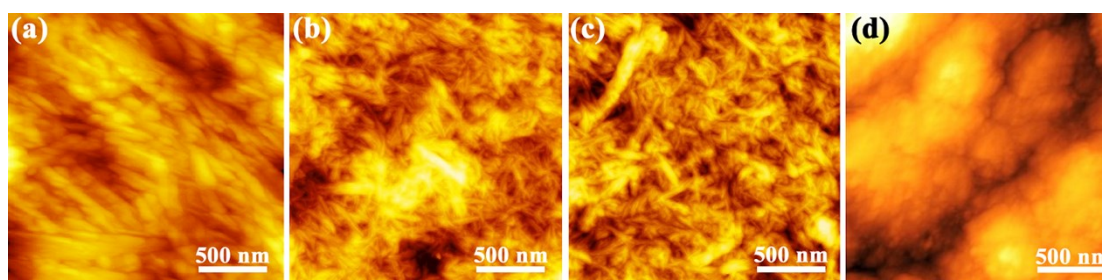


Figure S2. AFM images of CNC samples: (a) NC30%; (b) NC40%; (c) NC50%; (d) NC60%.

Table S2. Size distributions of CNC samples obtained at different TBPH concentrations^a

Sample	NC30%		NC40%		NC50%		NC60%	
	L (nm) ^b	D (nm) ^c						
Mean (nm)	158.3	11.9	89.3	8.8	41.6	8.2	30.5	6.9
SD (nm) ^d	55.9	3.5	21.9	2.7	9.7	2.3	8.8	2.1
Aspect ratio ^e	13.3		10.1		5.1		4.4	

^a Length and diameter data of 200 CNC particles in the TEM images were collected and analyzed for each sample in this table.

^b Length.

^c Diameter.

^d Standard deviation.

^e The ratio of length to diameter.

Table S3. Size distributions of CNC samples obtained at different temperatures and pulp CNC^a

Sample	NC40°C		NC50°C		NC60°C		Pulp CNC	
	L (nm) ^b	D (nm) ^c						
Mean (nm)	64.1	9.1	89.3	8.8	88.1	8.5	117.4	9.1
SD (nm) ^d	25.5	2.7	21.9	2.7	21.5	2.6	32.9	2.6
Aspect ratio ^e	7		10.1		10.4		12.9	

^a Length and diameter data of 200 CNC particles in the TEM images were collected and analyzed for each sample in this table.

^b Length.

^c Diameter.

^d Standard deviation.

^e The ratio of length to diameter.

TBPH concentration calibration

The initial nominal TBPH concentration provided by the manufacturer was 40 wt%, and it was dilute to 30 wt% with water and concentrated to 50 wt% and 60 wt% through vacuum concentration at room temperature. The TBPH solution was then titrated with 1 M hydrochloric acid as titrant and methyl orange as indicator to determine the actual concentration according to the literature,⁶ and the results are presented in Table S4.

Table S4. Actual concentration results of TBPH solution.

Nominal Concentration (wt%)	Actual concentration (wt%)
30	26.8±0.1
40	35.7±0.1
50	44.6±0.1
60	50.7±0.1

XRD results and peak deconvolution analysis

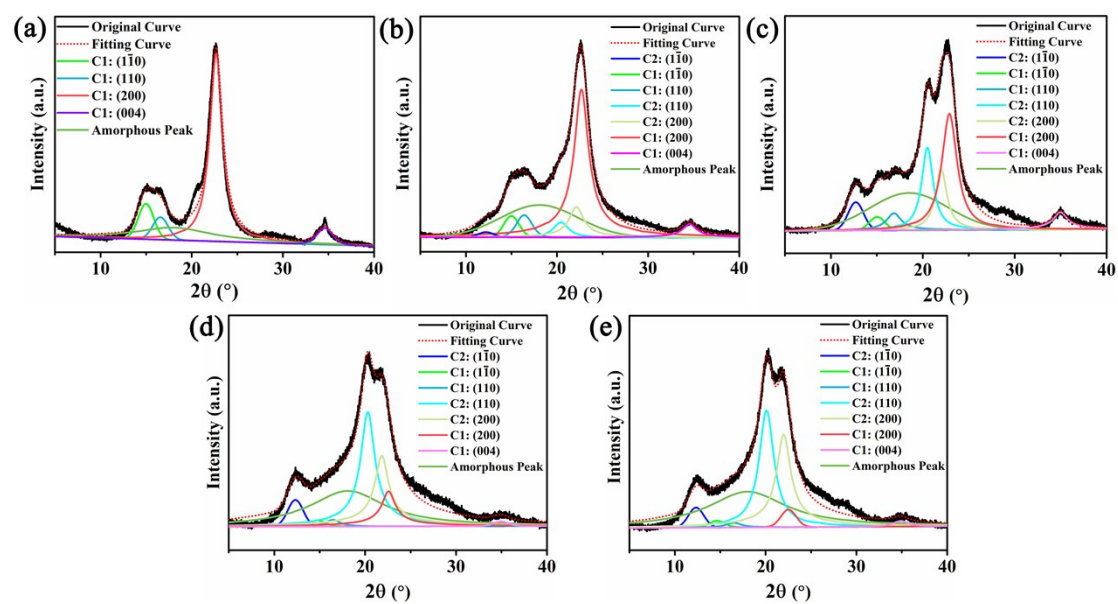


Figure S3. Peak deconvolution results of MCC and CNC obtained at different TBPH concentrations: (a) MCC; (b) NC30%; (c) NC40%; (d) NC50%; (e) NC60%.

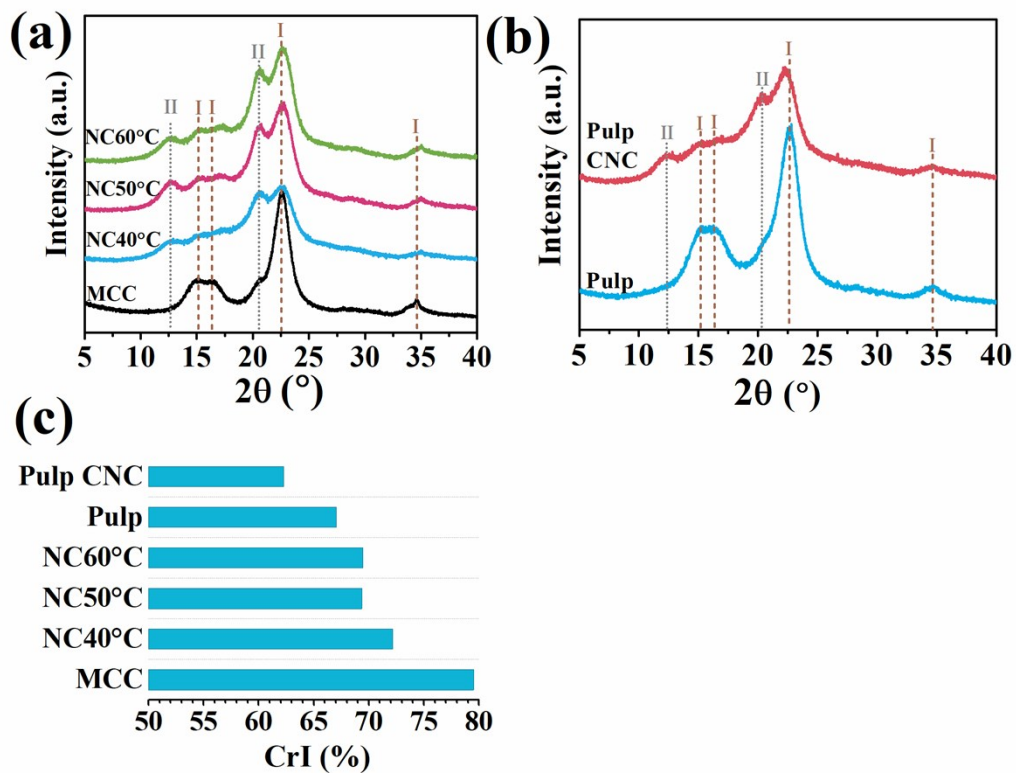


Figure S4. XRD patterns and crystallinity comparison: (a) XRD results of MCC and CNC obtained at different temperatures; (b) XRD results of pulp and pulp CNC; (c) Crystallinity (CrI) of MCC, pulp and different CNC samples.

FT-IR analysis

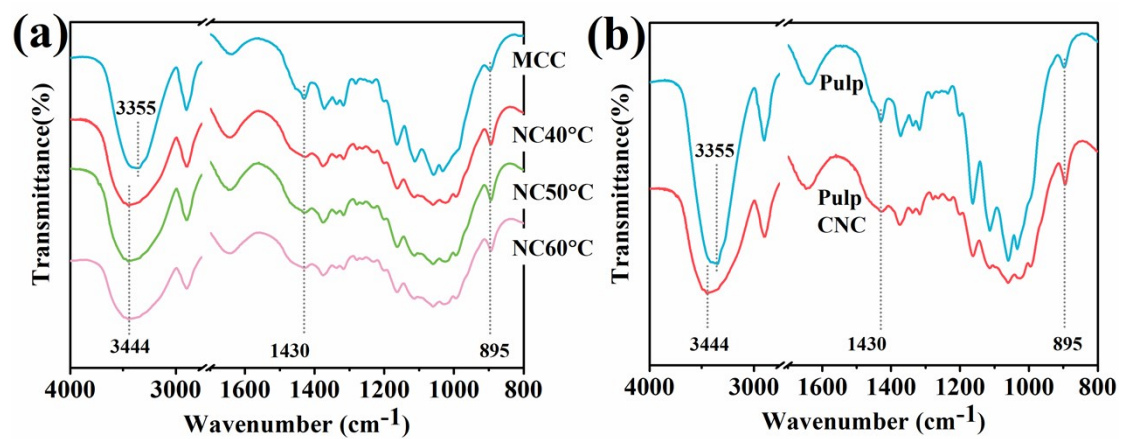


Figure S5. (a) FT-IR spectra of MCC and CNC obtained at different temperatures; (b) FT-IR spectra of pulp and pulp CNC.

Table S5. Peak assignment in FT-IR spectra of raw materials and CNCs⁷⁻¹⁰

Wavenumber (cm ⁻¹)	Assignment
3355-3468	O–H stretching vibration
2900-2921	C–H stretching vibration
1640-1645	O–H bending vibration of the adsorbed water
1420-1430	–CH ₂ –OH bending vibration
1372	C–H bending vibration
1317	–CH ₂ wagging vibration
1161	O–H wagging vibration; C–C ring breathing band
1112	C–O–C glycosidic ether band
1058	C–O–C pyranose ring stretching vibration
895	β-glycosidic linkages between glucose units in cellulose

Thermal stability analysis

Pulp and pulp CNC samples showed no significant difference in the extrapolated onset temperature (320 °C), while the temperature corresponding to the maximum decomposition rate of pulp was higher than that of pulp CNC (355 °C vs. 344 °C). The potential reason was that the molecular weight of pulp CNC was smaller than that of the raw material, which led to a decrease in the maximum degradation temperature.¹¹

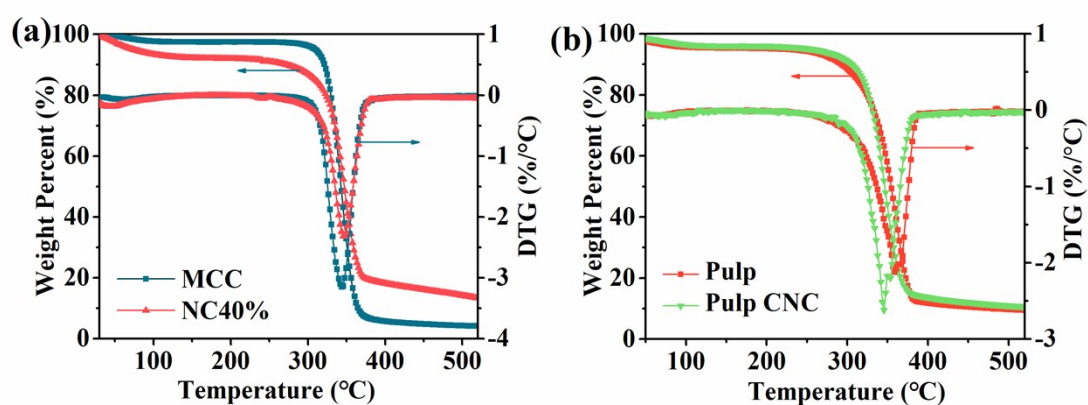


Figure S6. TG and DTG curves: (a) MCC and NC40%; (b) Pulp and pulp CNC.

Peak deconvolution analysis for MCC, regenerated cellulose, NC40%, and residue

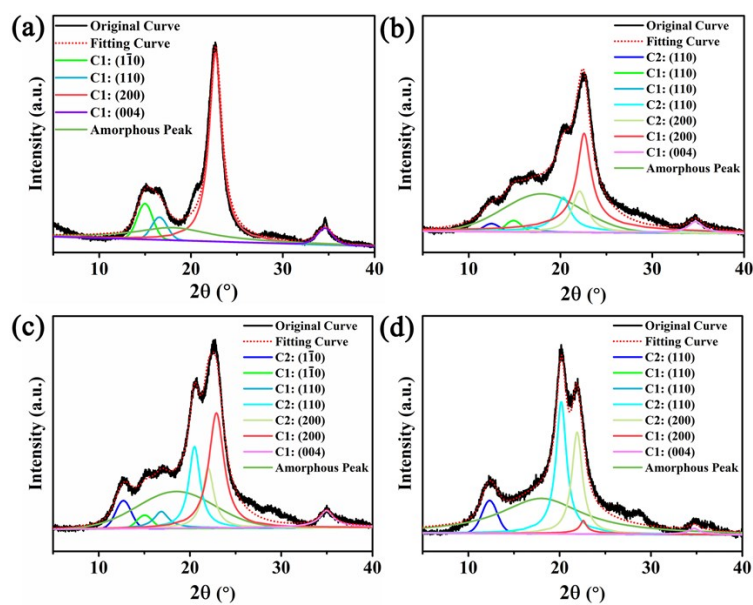


Figure S7. Peak deconvolution results of CNC obtained at different temperatures: (a) MCC; (b) Regenerated cellulose; (c) NC40%; (d) Residue.

Determination of reducing sugar concentration

DNS method was employed to determine the reducing sugar concentration of the enzymatic hydrolysate.¹² Firstly, the DNS solution was prepared as follows: 6.3 g DNS were dissolved in 262 mL 2 M sodium hydroxide solution, and then mixed with 500 mL hot water containing 182 g potassium sodium tartrate; subsequently, 5 g phenol and 5 g sodium sulfite were added to the solution, and the mixture was stirred to totally dissolve them; after cooling, the solution was diluted to 1000 mL with water, and stored in brown bottle for a week before use. Secondly, the reducing sugar standard curve was determined. Specific volumes of standard glucose solution (1mg/mL), DNS solution (0.05 M) and water were accurately added into eleven 25 mL graduated test tubes (numbered 0 to 10), respectively, as shown in Table S6. The mixed solution was heated in boiling water for 5 min, cooled to room temperature with cold water immediately, and diluted to 25 mL with deionized water. The absorbances of No. 1-10 samples were measured with SP-754 UV/Vis spectrophotometer (Shanghai Spectrophotometer Co., Ltd) at 540 nm with No. 0 sample as the control. Based on the above results, the standard curve was drawn and the regression equation was obtained with the absorbance as ordinate and glucose mass as abscissa, as shown in Figure S8.

Table S6. Reagent dosages for reducing sugar standard curve determination

Reagents	Test tube number										
	0	1	2	3	4	5	6	7	8	9	10
Standard glucose solution (mL)	0	0.2	0.4	0.6	0.8	1.0	1.2	1.4	1.6	1.8	2.0
Water (mL)	2.0	1.8	1.6	1.4	1.2	1.0	0.8	0.6	0.4	0.2	0
DNS solution (mL)	1.5	1.5	1.5	1.5	1.5	1.5	1.5	1.5	1.5	1.5	1.5
Glucose (mg)	0	0.2	0.4	0.6	0.8	1.0	1.2	1.4	1.6	1.8	2.0

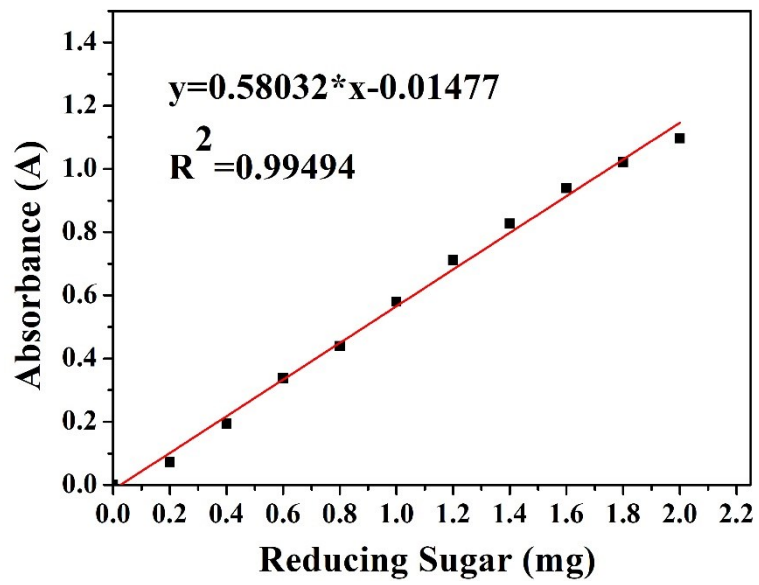


Figure S8. Reducing sugar standard curve

Determination of enzyme activity

The filter paper method was used for the enzyme activity determination of cellulase.¹³ Specific volumes of standard enzyme solution (2 mg/mL) and citric acid/sodium citrate buffer solution (0.05 M, pH 4.8) were accurately added into six 25 mL graduated test tubes (numbered 0 to 5), respectively, as shown in Table S7. The filter paper (approximately 50 mg) was put into No. 1-5 test tubes and fully immersed by the solution. The enzymatic hydrolysis was carried out at 50 °C for 1 h with an oscillating speed of 200 r/min, and the tube was quickly put in the boiling water for 10 min to inactivate the enzyme. After cooling and the addition of 1.5mL 0.05M DNS solution, the solution was heated in boiling water for 5 min. After rapid cooling, the solution was diluted to 25 mL with deionized water. No. 0 tube followed the same procedures while no filter paper was added. The absorbance of the solution was measured with SP-754 UV/Vis spectrophotometer (Shanghai Spectrophotometer Co., Ltd) at 540 nm with No. 0 tube as the control. The reducing sugar content were obtained according to the above reducing sugar standard curve, and the enzyme activity was calculated with Equation S1.

$$\text{Enzyme activity (FPU)} = 2 / (0.18 \times 60 \times W \times C)$$

(S1)

where W and C represent the amount and concentration of enzyme when the amount of the produced reducing sugar was 2 mg, respectively. The enzyme activity of the cellulase was 114 FPU/mg.

Table S7. Reagent dosages for enzyme activity determination

Reagents	Test tube number					
	0	1	2	3	4	5
2 mg/mL enzyme solution (mL)	0	0.6	0.7	0.8	0.9	1.0
0.05 M Buffer solution (mL)	2	1.4	1.3	1.2	1.1	1.0
Enzyme concentration (mg/mL)	0	0.6	0.7	0.8	0.9	1.0

References:

1. H. Kargarzadeh, I. Ahmad, I. Abdullah, A. Dufresne, S. Y. Zainudin and R. M. Sheltami, *Cellulose*, 2012, **19**, 855-866.
2. M. N. Nguyen, U. Kragl, D. Michalik, R. Ludwig and D. Hollmann, *ChemSusChem*, 2019, **12**, 3458-3462.
3. M. Abe, Y. Fukaya and H. Ohno, *Chem. Commun.*, 2012, **48**, 1808-1810.
4. Z. Pang, P. Wang and C. Dong, *Cellulose*, 2018, **25**, 7053-7064.
5. A. A. Silva and M. L. Laver, *Tappi J.*, 1997, **80**, 173-180.
6. B. B. Y. Lau, E. T. Luis, M. M. Hossain, W. E. S. Hart, B. Cencia-Lay, J. J. Black, T. Q. To and L. Aldous, *Bioresour. Technol.*, 2015, **197**, 252-259.
7. W. Xiao, W. Yin, S. Xia and P. Ma, *Carbohydr. Polym.*, 2012, **87**, 2019-2023.
8. Q. Gao, X. Shen and X. Lu, *Carbohydr. Polym.*, 2011, **83**, 1253-1256.
9. Y. Hu, I. N. Oduro, Y. Huang and Y. Fang, *J. Anal. Appl. Pyrolysis*, 2016, **120**, 416-422.
10. A. Mandal and D. Chakrabarty, *Carbohydr. Polym.*, 2011, **86**, 1291-1299.
11. H. Z. Chen, N. Wang and L. Y. Liu, *J. Chem. Technol. Biotechnol.*, 2012, **87**, 1634-1640.
12. R. F. Hu, L. Lin, T. J. Liu, P. Ouyang, B. H. He and S. J. Liu, *J. Biobased Mater. Bioenerg.*, 2008, **2**, 156-161.
13. T. K. Ghose, *Pure Appl. Chem.*, 1987, **59**, 257-268.